Binuclear and Starburst Organoplatinum(II) Complexes of 2,2‘-Dipyridylamino Derivative Ligands: Structures, Fluxionality, and Luminescence

ARTICLE *in* ORGANOMETALLICS · JULY 2003

Impact Factor: 4.13 · DOI: 10.1021/om030262k

Binuclear and Starburst Organoplatinum(II) Complexes of 2,2′-Dipyridylamino Derivative Ligands: Structures, Fluxionality, and Luminescence

Qin-De Liu, Wen-Li Jia, Gang Wu, and Suning Wang*

Department of Chemistry, Queen's University, Kingston, Ontario, K7L 3N6, Canada

Received April 10, 2003

New binuclear and starburst trinuclear organoplatinum complexes based on 2,2′-dipyridylamino (dpa) derivative ligands, Pt_2Ph_4(bab), bab = 1,4-bis(2,2′-dipyridylamino)-benzene, **1**, Pt_2Ph_4(babp), babp = 4,4′-bis(2,2′-dipyridylamino)biphenyl, **2**, Pt_3Ph_6(tab), tab = 1,3,5-tris(2,2′-dipyridylamino)benzene, **3**, Pt_3Ph_6(tat), tat = 2,4,6-tris(2,2′-dipyridylamino)-1,3,5-triazine, **4**, Pt_3Ph_6(tapb), tapb = 1,3,5-tris[*p*-(2,2′-dipyridylamino)phenyl]-benzene, **5**, Pt_3Ph_6(tapt), tapt = 2,4,6-tris[*p*-(2,2′-dipyridylamino)phenyl]-1,3,5-triazine, **6**, Pt_3Ph_6(tabpb), tabpb = 1,3,5-tris{4′-[4″-(2,2′-dipyridylamino)]biphenyl}benzene, **7**, and Pt_3Ph_6(tabpt), tabpt = 1,3,5-tris{4′-[4″-(2,2′-dipyridylamino)]biphenyl}benzene, **8**, were synthesized by the reaction of $[PtPh_2(SMe_2)]_n$ with the corresponding chelate ligand. The structures of complexes **1**−**5** and **8** were determined by single-crystal X-ray diffraction. All eight complexes have phosphorescent emissions in the blue/green region at 77 K, attributed to ligand-centered $\pi \rightarrow \pi^*$ transitions. Ligand-based fluorescent emission was also detected for complexes **5**, **6**, and **8**. Complexes **1**−**8** display versatile structures in the solid state. Complex **4** was found to be fluxional in solution. The key factors that influence the structures of the complexes in solution and the solid state are the degree of conjugation of the amino nitrogen lone pair electrons of the dpa unit with the central aromatic linker and intramolecular nonbonding interactions.

Introduction

Luminescent organoplatinum compounds have attracted much recent attention due to their potential applications in many areas such as photosensitization,[1] chemical sensing,[2] and supramolecular photosensitization.[3] The potential applications of phosphorescent platinum complexes as emitters in organic light-emitting devices (OLEDs) further motivated the research efforts in luminescent organoplatinum compounds.[4] It has been demonstrated recently that the Pt(II) center in organoplatinum complexes plays a key role in promoting singlet−triplet state mixing, hence enhancing phosphorescent emission of the organic chromophores in the complexes. OLEDs using phosphorescent Pt(II) complexes have been demonstrated. Most previously known luminescent platinum complexes are based on square-planar cycloplatinated complexes that involve a tridentate chelate ligand and an ancillary ligand.[5] The emission of these cycloplatinated complexes usually originates from metal-to-ligand charge transition (MLCT) or metal−metal-to-ligand charge transition (MMLCT). Stable luminescent multinuclear platinum complexes with a neutral bidentate-chelate ligand are scarce. Ligands (L) with two chelating nitrogen donors, such as 2,2′-dipyridylamine or phenanthrene, can easily bidentately coordinate to platinum(II) centers, forming neutral $PtLR_2$ complexes, where R is a −1 charged

(1) (a) Houlding, V. H.; Miskowski, V. M. *Coord. Chem. Rev.* **1991**, *111*, 145. (b) Pettijohn, C. N.; Jochnowitz, E. B.; Chuong, B.; Nagle, J. K.; Vogler, A. *Coord. Chem. Rev.* **1998**, *171*, 85. (c) Yersin, H.; Humbs, W.; Strasser, J. *Coord. Chem. Rev.* **1997**, *159*, 325. (d) Paw, W.; Cummings, S. D.; Mansour, M. A.; Connick, W. B.; Gieger, D. K.; Eisenberg, R. *Coord. Chem. Rev.* **1998**, *171*, 125. (e) McGarrah, J. E.; Kim, Y. J.; Hissler, M.; Eisenberg, R. *Inorg. Chem.* **2001**, *40*, 4510.

(2) (a) Chassot, L.; Müller, E.; von Zelewsky, A. *Inorg. Chem.* **1984**, *23*, 4249. (b) Sandrini, D.; Maestri, M.; Balzani, V.; Chassot, L.; von Zelewsky, A. *J. Am. Chem. Soc.* **1987**, *109*, 3107. (c) Vogler, A.; Kunkely, H. *Coord. Chem. Rev.* **1998**, *177*, 81. (d) Wan, K. T.; Che, C. M.; Cho, K. C. *J. Chem. Soc., Dalton Trans.* **1991**, 1077. (e) Che, C. M.; Wan, K. T.; He, L. T.; Poon, C. K.; Yam, V. W. W. *J. Chem. Soc., Dalton Trans.* **1989**, 2011. (f) Wan, K. T.; Che, C. M. *J. Chem. Soc., Chem. Commun.* **1990**, 140.

(3) (a) Wu, L. Z.; Cheung, T. C.; Che, C. M.; Cheung, K. K.; Lam, M. H. H. *Chem. Commun.* **1998**, 1127. (b) Lee, W. W. S.; Wong, K. Y.; Li, X. M. *Anal. Chem.* **1993**, *65*, 255. (c) Cusumano, M.; Di Pietro, M. L.; Giannetto, A. *Inorg. Chem.* **1999**, *38*, 1754. (d) Wong, K. H.; Chan, M. C. W.; Che, C. M. *Chem.-Eur. J.* **1999**, *10*, 2845.

(4) (a) Baldo, M. A.; O'Brien, D. F.; You, Y.; Shoustikov, A.; Sibley, S.; Thompson, M. E.; Forrest, S. R. *Nature* **1998**, *395*, 151. (b) Kwong, R. C.; Sibley, S.; Dubovoy, T.; Baldo, M.; Forrest, S. R.; Thompson, M. E. *Chem. Mater.* **1999**, *11*, 3709. (c) Kwong, R. C.; Lamansky, S.; Thompson, M. E. *Adv. Mater.* **2000**, *12*, 1134. (d) Lu, W.; Mi, B. X.; Chan, M. C. W.; Hui, Z.; Zhu, N.; Lee, S. T.; Che, C. M. *Chem. Commun.* **2002**, 206. (f) Liu, Q.; Thorne, L.; Kozin, I.; Song, D.; Seward, C.; D'Iorio, M.; Tao, Y.; Wang, S. *J. Chem. Soc., Dalton Trans.* **2002**, 3234.

(5) For some newest examples: (a) McMillin, D. R.; Moore, J. J. *Coord. Chem. Rev.* **2002**, *229*, 113, and references therein. (b) Field, J. S.; Haines, R. J.; McMillin, D. R.; Summerton, G. C. *J. Chem. Soc., Dalton Trans.* **2002**, 1369. (c) Moore, J. J.; Nash, J. J.; Fanwick, P. E.; McMillin, D. R. *Inorg. Chem.* **2002**, *41*, 6387. (d) Yutaka, T.; Mori, I.; Kurihara, M.; Mizutani, J.; Tamai, N.; Kawai, T.; Irie, M.; Nishihara, H. *Inorg. Chem.* **2002**, *41*, 7143. (e) Yang, Q. Z.; Wu, L. Z.; Wu, Z. X.; Zhang, L. P.; Tung, C. H. *Inorg. Chem.* **2002**, *41*, 5653. (f) Yam, V. W. W.; Wong, K. M. C.; Zhu, N. *J. Am. Chem. Soc.* **2002**, *124*, 6506. (g) Yam, V. W. W.; Hui, C. K.; Wong, K. M. C.; Zhu, N.; Cheung, K. K. *Organometallics* **2002**, *21*, 4326. (h) Che, C. M.; Zhang, J. L.; Lin, L. R. *Chem. Commun.* **2002**, 2556. (i) Che, C. M.; Fu, W. F.; Lai, S. W.; Hou, Y. J.; Liu, Y. L. *Chem. Commun.* **2003**, 118. (j) Lu, W.; Zhu, N.; Che, C. M. *Chem. Commun.* **2002**, 900. (k) Hui, C. K.; Chu, B. W. K.; Zhu, N.; Yam, V. W. W. *Inorg. Chem.* **2002**, *41*, 6178. (l) Michalec, J. F.; Bejune, S. A.; Cuttell, D. G.; Summerton, G. C.; Gertenbach, J. A.; Field, J. S.; Haines, R. J.; McMillin, D. R. *Inorg. Chem.* **2001**, *40*, 2193.

10.1021/om030262k CCC: $25.00
Publication on Web 07/25/2003

Scheme 1

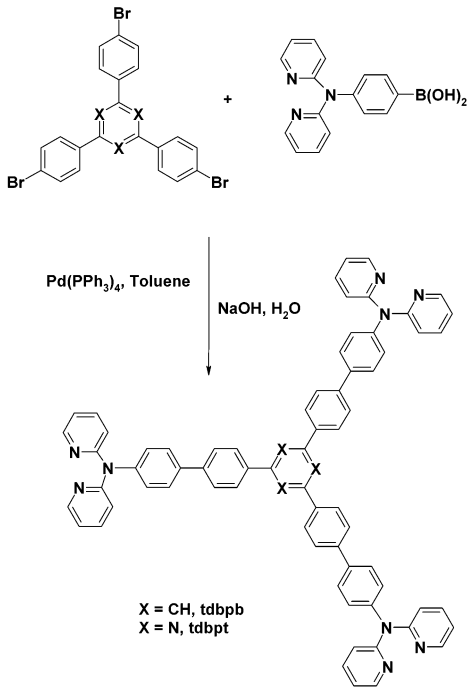

ligand.[1] We have previously reported a series of linear linker ligands (bab and babp) and starburst ligands (tab, tat, tapb, and tapt) containing 2,2′-dipyridylamino functional groups (Scheme 1). This class of molecules has been found to have good film-forming properties and to be good blue emitters for OLEDs.[6a] In addition, we have observed this class of molecules are also effective ligands for the formation of luminescent lanthanides, and transition metal complexes, that display intriguing structural features and chemical sensing capabilities.[6b−d] In continuation of this work, we have synthesized two new starburst ligands (tabpb and tabpt) and have investigated systematically the properties of organoplatinum(II) complexes containing the new ligands and the previously reported linear and starburst ligands of dpa derivative. Herein we report the syntheses, crystal structures, and luminescent properties of these new compounds.

Experimental Section

All starting materials were purchased from Aldrich Chemical Co. and used without further purification. Solvents were freshly distilled over appropriate drying reagents. ^{1}H NMR were recorded on a Bruker Advance 300 MHz spectrometer. ^{13}C NMR were recored on a Bruker Advance 500 MHz spectrometer operated at 125 MHz. Excitation and emission spectra were obtained with a Photon Technologies International QuantaMaster Model C-60 spectrometer. Emission lifetime was measured on a Photon Technologies International Phosphorescent lifetime spectrometer, Timemaster C-631F equipped with a Xenon flash lamp, and digital emission photon multiplier tube using a band pathway of 5 nm for excitation and 2 nm for emission. UV−vis spectra were recorded on a Hewlett-Packard 8562A diode array spectrophotometer. Thermogravometric analysis (TGA) was performed using a Perkin-Elmer TGA 7 analyzer. Elemental analyses were performed by Canadian Microanalytical Service Ltd., Delta, British Columbia, Canada. The syntheses of the ligands bab, babp, tab, tat, tapb, and tapt were achieved by previously published procedures.[6] The Pt(II) starting material $[PtPh_2(SMe_2)]_n$ (n = 2 or 3) was synthesized using a procedure reported in the literature.[7]

1,3,5-Tris{4′-[4″-(2,2′-dipyridylamino)]biphenyl}benzene (tabpb). A mixture of tris(*p*-bromophenyl)benzene (0.44 g, 0.8 mmol) and $Pd(PPh_3)_4$ (0.04 g) was suspended in toluene (60 mL) and stirred for 10 min. Then *p*-(2,2′-dipyridylamino)-phenylboronic acid (1.4 g, 4.81 mmol) in 20 mL of EtOH and NaOH (0.6 g) in 20 mL of H_2O were subsequently added. The mixture was stirred and refluxed for 36 h and allowed to cool to room temperature. The aqueous layer was separated and extracted with CH_2Cl_2 (3 × 25 mL). The combined organic layers were dried over $MgSO_4$, and the solvents were evaporated under reduced pressure. Purification of the crude product by column chromatography (THF/hexane, 3:1) afforded tabpd as a white solid in 54% yield. Mp: 146−148 °C. ^{1}H NMR (CD_2Cl_2, δ, ppm): 8.33(dd, 6H, J = 4.8, 1.2 Hz), 7.99(s, 3H), 7.91(d, 6H, J = 8.4 Hz), 7.82(d, 6H, J = 8.4 Hz), 7.74(d, 6H, J = 8.7 Hz), 7.65(ddd, 6H, J = 8.4, 7.2, 1.8 Hz), 7.29(d, 6H, J = 8.4 Hz), 7.12(d, 6H, J = 8.4 Hz), 7.02(ddd, 6H, J = 7.3, 4.8, 0.9 Hz). ^{13}C NMR in (CD_2Cl_2, δ, ppm): 158.5, 148.8, 145.1, 142.1, 140.1, 137.8, 137.7, 136.2, 128.3, 128.1, 127.9, 127.8, 125.8, 118.7, 117.5. Anal. Calcd for $C_{72}H_{51}N_9 \cdot H_2O$: C 81.59, H 5.00, N 11.90. Found: C 81.54, H 5.48, N 11.38.

2,4,6-Tris{4′-[4″-(2,2′-dipyridylamino)]biphenyl}-1,3,5-triazine (tabpt). In the same manner described for tabpb, the reaction of tris(*p*-bromophenyl)benzene (0.67 g, 1.23 mmol) with *p*-(2,2′-dipyridylamino)phenylboronic acid (1.87 g, 6.18 mmol) catalyzed by $Pd(PPh_3)_4$ (0.06 g) and NaOH (0.4 g) provided tabpt as a light yellow-green solid in 56% yield. Mp: 274−276 °C. ^{1}H NMR in (CD_2Cl_2, δ, ppm): 8.92(d, 6H, J = 8.4 Hz), 8.35(dd, 6H, J = 4.8, 1.2 Hz), 7.91(d, 6H, J = 8.4 Hz), 7.79(d, 6H, J = 8.4 Hz), 7.68(ddd, 6H, J = 8.4, 7.2, 1.8 Hz), 7.32(d, 6H, J = 8.4 Hz), 7.12(d, 6H, J = 8.4 Hz), 7.02(ddd, 6H, J = 7.2, 5.1, 0.9 Hz). ^{13}C NMR in (CD_2Cl_2, δ, ppm): 158.7, 149.1, 146.0, 145.1, 138.2, 137.5, 135.8, 130.2, 128.9, 128.0, 127.7, 126.1, 119.1, 117.8. Anal. Calcd for $C_{69}H_{48}N_{12} \cdot 1/2THF$: C 78.89, H 4.81, N 15.56. Found: C 79.31, H 4.60, N 16.05.

Pt_2Ph_4(bab) (1). Benzene (5 mL) and a solution of $[PtPh_2(SMe_2)]_n$ (99 mg, 0.24 mmol Pt) in 10 mL of THF were successfully layered upon a solution of 1,4-bis(2,2′-dipyridylamino)benzene (bab, 50 mg, 0.12 mmol) in 5 mL of CH_2Cl_2. This three-layered solution was allowed to stand at room temperature. The Pt-containing solution sank through the benzene layer and into the CH_2Cl_2 layer slowly, producing **1** as colorless crystals after several days (96 mg, 72%). Compound **1** is insoluble in any organic solvent. NMR spectra could not be obtained. Anal. Calcd for $C_{50}H_{40}N_6Pt_2$: C 53.86, H 3.62, N 7.53. Found: C 53.67, H 3.64, N 7.32.

Pt_2Ph_4(babp) (2). 4,4′-Bis(2,2′-dipyridylamino)biphenyl (babp, 50 mg, 0.10 mmol) and $[PtPh_2(SMe_2)]_n$ (84 mg, 0.20 mmol Pt) were dissolve in 5 mL of THF/CH_2Cl_2 (1:1). After being stirred for 10 min, the solution was filtered, and 2 mL of toluene was added slowly to the filtrate and successfully layered upon the solution. Solvents were allowed to diffuse and evaporate slowly over 2 days at ambient temperature, producing light yellow crystals of **2** (85 mg, 66%). ^{1}H NMR (CD_2Cl_2, δ, ppm): 8.47(ddd, 4H, J = 5.6, 1.9, 0.6 Hz, Py), 7.95-(ddd, 4H, J = 8.1, 7.5, 1.9 Hz, Py), 7.75(d, 4H, J = 8.7 Hz, middle Ph), 7.67(ddd, 4H, J = 8.1, 1.2, 0.6 Hz, Py), 7.38(dd, 8H, J = 7.8, 1.4 Hz, $^3J_{Pt-H}$ = 70.8 Hz, Ph), 7.23(d, 4H, J = 8.8 Hz, central Ph), 7.14(ddd, 4H, J = 7.4, 5.6, 1.3 Hz, Py), 6.89(t,

(6) (a) Pang, J.; Tao, Y.; Freiberg, S.; Yang, X. P.; D'Iorio, M.; Wang, S. *J. Mater. Chem*. **2002**, *12*, 206. (b) Yang, W. Y.; Chen, L.; Wang, S. *Inorg. Chem*. **2001**, *40*, 507. (c) Seward, C.; Pang, J.; Wang, S. *Eur. J. Inorg. Chem*. **2002**, 1390. (d) Pang, J.; Marcotte, E. J.-P.; Seward, C.; Brown, R. S.; Wang, S. *Angew. Chem., Int. Ed*. **2001**, *40*, 4042.

(7) (a) Scott, J. D.; Puddephatt, R. J. *Organometallics* **1983**, *2*, 1643. (b) Hill, G. S.; Irwin, M. J.; Levy, C. J.; Rendina, L. M.; Puddephatt, R. J. *Inorg. Synth*. **1998**, *32*, 149. (c) Song, D.; Wang, S. *J. Organomet. Chem*. **2002**, *648*, 302.

8H, $J = 7.5$ Hz, Ph), 6.77(tt, 4H, $J = 7.8$, 1.5 Hz, Ph). ^{13}C NMR (CD_2Cl_2, δ, ppm): 153.6, 151.9, 144.9, 144.6, 139.6, 138.6, 136.2, 128.5, 126.6, 124.0, 123.8, 121.8, 120.3. Anal. Calcd for $C_{56}H_{44}N_6Pt_2$·THF: C 57.00, H 4.12, N 6.65. Found: C 56.55, H 4.13, N 6.60.

Pt_3Ph_6(tab) (3). A mixture of 1,3,5-tris(2,2′-dipyridylamino)benzene (tab, 50 mg, 0.085 mmol) and $[PtPh_2(SMe_2)]_n$ (107 mg, 0.26 mmol Pt) was dissolved in 10 mL of THF, and the solution was stirred at room temperature. A white solid precipitated after 30 min. The solution was stirred for another 5 h at room temperature, and the white precipitate was collected by filtration. The solid was dissolved in 30 mL of CH_2Cl_2. Toluene (10 mL) was layered upon the solution. Solvents were allowed to diffuse and evaporate slowly over several days at ambient temperature, producing a white microcrystalline solid of **3** (90 mg, 65%). ^{1}H NMR (CD_2Cl_2, δ, ppm): 8.39(dd, 6H, $J = 5.5$, 1.3 Hz, Py), 7.77(td, 6H, $J = 7.3$, 1.7 Hz, Py), 7.70(d, 6H, $J = 7.3$ Hz, Py), 7.32(dd, 12H, $J = 7.9$, 1.4 Hz, $J_{Pt-H} = 69.7$ Hz, Ph), 7.06(ddd, 6H, $J = 7.2$, 5.7, 1.4 Hz, Py), 6.89−6.77(m, 18H, Ph), 6.48(s, 3H, central Ph). ^{13}C NMR (CD_2Cl_2, δ, ppm): 152.7, 152.0, 148.8, 144.3, 139.8, 138.6, 127.0, 124.5, 124.3, 121.9, 105.1. Anal. Calcd for $C_{72}H_{57}N_9Pt_3$·0.5CH_2Cl_2: C 52.31, H 3.46, N 7.52. Found: C 52.21, H 3.02, N, 7.57.

Pt_3Ph_6(tat) (4). In the same manner described for **3**, the reaction of 2,4,6-tris(2,2′-dipyridylamino)-1,3,5-triazine (tat, 50 mg, 0.085 mmol) with $[PtPh_2[SMe_2)]_n$ (107 mg, 0.26 mmol Pt) provided **4** as colorless crystals (86 mg, 62%). ^{1}H NMR (CD_2Cl_2, 243 K, δ, ppm,): 8.29 (d, 2H, $J = 5.0$ Hz), 8.10 (d, 2H, $J = 5.0$ Hz), 8.03 (d, 2H, $J = 5.0$ Hz), 7.88 (t, 2H, $J = 8.5$ Hz), 7.80 (d, 2H, $J = 8.5$ Hz), 7.74 (d, 2H, $J = 8.0$ Hz), 7.39−7.59 (m, 18 H), 7.12 (t, 2H, $J = 6.5$ Hz), 6.75−7.04 (m, 22 H). Anal. Calcd for $C_{69}H_{54}N_{12}Pt_3$·0.5CH_2Cl_2: C 49.90, H 3.29, N 9.98. Found: C 49.76, H 3.42, N 10.01.

Pt_3Ph_6(tapb) (5). In the same manner described for **1**, the reaction of 1,3,5-tris[*p*-(2,2′-dipyridylamino)phenyl]benzene (tapb, 50 mg, 0.061 mmol) with $[PtPh_2(SMe_2)]_n$ (76 mg, 0.184 mmol Pt) provided **5** as colorless crystals (67 mg, 59%). ^{1}H NMR (DMSO-d_6, δ, ppm): 8.27(d, 6H, $J = 6.6$ Hz, Py), 8.19(t, 6H, $J = 6.9$ Hz, Py), 7.98−7.92(m, 15H, Py, arm Ph, central Ph), 7.37(t, 6H, $J = 6.6$ Hz, Py), 7.26(d, 12H, $J = 7.0$ Hz, Ph), 7.17(d, 6H, $J = 8.7$ Hz, arm Ph), 6.77(t, 12H, 7.2 Hz, Ph), 6.64-(t, 6H, $J = 7.1$ Hz, Ph). ^{13}C NMR (DMSO-d_6, δ, ppm): 158.4, 149.1, 147.5, 145.4, 141.9, 138.8, 137.0, 129.1, 128.1, 128.0, 123.9, 119.4, 117.8. (two quaternary carbons hidden). Anal. Calcd for $C_{90}H_{69}N_9Pt_3$: C 58.06, H 3.74, N 6.77. Found: C 58.54, H 3.99, N 6.44.

Pt_3Ph_6(tapt) (6). In the same manner described for **1**, the reaction of 2,4,6-tris[*p*-(2,2′-dipyridylamino)phenyl]-1,3,5-triazine (tapt, 50 mg, 0.061 mmol) with $[PtPh_2(SMe_2)]_n$ (76 mg, 0.184 mmol Pt) provided **6** as a light yellow solid (62 mg, 55%). ^{1}H NMR (DMSO-d_6, δ, ppm): 8.73(d, 6H, $J = 8.7$ Hz, arm Ph), 8.26−8.32(m, 12 H, Py), 8.08(d, 6H, $J = 7.3$ Hz, Py), 7.50(t, 6H, $J = 6.6$ Hz, Py), 7.21(d, 12H, $J = 7.5$ Hz, Ph), 6.89(d, 6H, $J = 8.8$ Hz, arm Ph), 6.76(t, 12H, $J = 7.3$ Hz, Ph), 6.63(t, 6H, $J = 7.3$ Hz, Ph). ^{13}C NMR could not be obtained. Anal. Calcd for $C_{87}H_{66}N_{12}Pt_3$: C 56.04, H 3.54, N 9.02. Found: C 56.36, H 3.73, N 8.87.

Pt_3Ph_6(tabpb) (7). In the same manner described for **2**, the reaction of 1,3,5-tris{4′-[4″-(2,2′-dipyridylamino)]biphenyl}-benzene (tabpb, 50 mg, 0.048 mmol) with $[PtPh_2(SMe_2)]_n$ (60 mg, 0.146 mmol Pt) provided **7** as a yellow microcrystalline solid (54 mg, 54%). ^{1}H NMR (CD_2Cl_2, δ, ppm): 8.49(dd, 6H, $J = 5.5$, 1.4 Hz, Py), 7.99(s, 3H, central Ph), 7.97(td, 6H, $J = 7.6$, 1.6 Hz, Py), 7.91(d, 6H, $J = 8.5$ Hz, arm Ph), 7.84(d, 6H, $J = 8.4$ Hz, arm Ph), 7.81(d, 6H, $J = 8.7$ Hz, arm Ph), 7.69(d, 6H, $J = 7.8$ Hz, Py), 7.39(dd, 12H, $J = 7.6$, 1.2 Hz, Ph), 7.24-(d, 6H, $J = 8.8$ Hz, arm Ph), 7.15(ddd, 6H, $J = 7.3$, 5.7, 1.3 Hz, Py), 6.90(t, 12H, $J = 7.5$ Hz, Ph), 6.78(tt, 6H, 7.3, 1.2 Hz, Ph). ^{13}C NMR (CD_2Cl_2, δ, ppm): 153.3, 151.9, 145.2, 144.6, 142.3, 139.8, 139.6, 138.6, 136.3, 129.4, 128.6, 128.5, 128.2, 127.6, 126.9, 124.2, 123.9, 121.8, 119.9. Anal. Calcd for $C_{108}H_{81}N_9Pt_3$·0.5CH_2Cl_2: C 61.11, H 3.88, N 5.91. Found: C 60.80, H 4.11, N 5.43.

Pt_3Ph_6(tabpt) (8). In the same manner described for **2**, the reaction of 2,4,6-tris{4′-[4″-(2,2′-dipyridylamino)]biphenyl}-1,3,5-triazine (tabpt, 50 mg, 0.048 mmol) with $[PtPh_2(SMe_2)]_n$ (60 mg, 0.146 mmol Pt) provided **8** as yellow crystals (61 mg, 61%). ^{1}H NMR (CD_2Cl_2, δ, ppm): 8.94(d, 6H, $J = 8.6$ Hz, arm Ph), 8.51(dd, 6H, $J = 5.6$, 1.6 Hz, Py), 8.00(td, 6H, $J = 7.6$, 1.8 Hz, Py), 7.93(d, 6H, $J = 8.6$ Hz, arm Ph), 7.86(d, 6H, $J = 8.8$ Hz, arm Ph), 7.72(d, 6H, $J = 7.6$ Hz, Py), 7.38(dd, 12H, $J = 7.8$, 1.3 Hz, Ph), 7.17−7.22(m, 12H, Py and arm Ph), 6.90-(t, 12H, $J = 7.5$ Hz, Ph), 6.77(tt, 6H, $J = 7.5$, 1.3 Hz, Ph). ^{13}C NMR (CD_2Cl_2, δ, ppm): 153.3, 152.0, 146.0, 144.6, 144.4, 139.7, 138.6, 135.5, 135.4, 129.9, 128.9, 127.3, 126.9, 124.7, 124.3, 121.9, 118.9 (one quaternary carbon hidden). Anal. Calcd for $C_{105}H_{78}N_{12}Pt_3$: C 60.25, H 3.76, N 8.03. Found: C 60.11, H 3.74, N 7.71.

X-ray Crystallographic Analysis. Single crystals of **1**−**5** and **8** were obtained and characterized by X-ray diffraction analysis. Crystals of **1**−**3** were mounted on glass fibers for data collection, while those of **4**, **5**, and **8** were sealed into thin-walled glass capillaries for structure determination. Data were collected on a Siemens P4 single-crystal X-ray diffractometer with a Smart CCD-1000 detector and graphite-monochromated Mo Kα radiation, operating at 50 kV and 35 mA at 25 °C. The data collection ranges over the 2θ ranges are 4.10−56.6° for **1**, 4.44−56.6° for **2** and **3**, 3.54−56.8° for **4**, 4.18−56.7° for **5**, and 2.60−56.8° for **8**. No significant decay was observed for all samples except **3** and **8**, which decayed substantially due to the loss of solvent molecules in the lattice. Data were processed on a PC using the Bruker SHELXTL software package[8] (version 5.10) and are corrected for Lorentz and polarization effects. Complexes **1**−**3** crystallize in the triclinic space group $P\bar{1}$, and the molecules of **1** and **2** possess an inversion center. The crystals of **4** and **5** belong to the monoclinic space group $P2_1/c$, while complex **8** crystallizes in the C-centered monoclinic space group $C2/c$. All structures were solved by direct methods. All non-hydrogen atoms in complexes **1**, **2**, **4**, and **5** except the solvent molecules, and a few carbon atoms in complex **4**, were refined anisotropically. The quality of the crystal data of **3**−**5** and **8** is poor due to the presence of disordered solvent molecules and the thin plate crystals. Crystals of **3** and **8** lose crystal lattice solvent molecules rapidly. In addition, compounds **3** and **8** produce only small and thin crystals, which diffract poorly. The solvent molecules in **8** were only partially resolved and refined. Consequently, only the platinum and some of the non-hydrogen atoms in **3** and **8** were refined anisotropically. Due to the poor quality of data, some of the terminal phenyl groups in **3** and **8** had to be refined as rigid bodies in order to obtain meaningful Pt−C bond distances. All hydrogen atoms except those of the disordered solvent molecules were calculated, and their contributions in structural factor calculations were included. The crystallographic data are given in Table 1. Selected bond lengths and angles are listed in Table 2.

Results and Discussions

Syntheses and Characterization of Ligands tdbpb and tdbpt and Compounds 1−8. All free ligands except the two largest starburst molecules tdbpb and tdbpt have been reported previously by our group. The new tdbpb and tdbpt ligands were synthesized in good yields using the Suzuki coupling procedures[9]

(8) *SHELXTL NT*, Crystal Structure Analysis Package, Version 5.10; Bruker AXS, Analytical X-ray System: Madison, WI, 1999.

(9) (a) Miyaura, N. *Adv. Metal-Org. Chem.* **1998**, *6*, 187, and references therein. (b) Suzuki, A. *J. Organomet. Chem.* **1999**, *576*, 147, and references therein.

Table 1. Data Collection and Processing Parameters for 1−5 and 8

	1	2	3	4	5	8
formula	$C_{50}H_{40}N_6Pt_2$	$C_{56}H_{44}N_6Pt_2$·THF	$C_{72}H_{57}N_9Pt_3$·5.4C_6H_6	$C_{69}H_{54}N_{12}Pt_3$·CH_2Cl_2·2C_7H_8	$C_{90}H_{69}N_9Pt_3$·2THF·0.5C_6H_6	$C_{105}H_{78}N_{12}Pt_3$·1.5C_7H_8
fw	1115.06	1263.26	2055.32	1905.71	2045.07	2231.26
space group	$P\bar{1}$	$P\bar{1}$	$P\bar{1}$	$P2_1/c$	$P2_1/c$	$C2/c$
a/Å	9.798(2)	8.0561(12)	14.077(4)	15.538(5)	20.421(5)	40.667(19)
b/Å	10.461(3)	9.7483(15)	18.207(5)	17.448(5)	22.248(5)	19.689(8)
c/Å	10.546(3)	17.006(3)	19.435(5)	28.578(9)	19.465(5)	33.039(15)
α/deg	72.401(4)	103.331(3)	63.920(5)	90	90	90
β/deg	74.464(4)	102.001(3)	84.685(5)	100.152(9)	95.587(4)	122.099(7)
γ/deg	80.902(4)	97.128(3)	76.713(4)	90	90	90
V/Å^3	989.2(4)	1250.2(3)	4354(2)	7626(4)	8801(4)	22 140(17)
Z	1	1	2	4	4	8
D_c/g cm^{-3}	1.872	1.678	1.568	1.660	1.543	1.323
μ/mm^{-1}	7.108	5.637	4.861	5.612	4.811	3.785
$2\theta_{max}$/deg	56.62	56.60	56.76	56.78	56.70	56.78
no. of reflns measd	7112	9132	25837	52591	61777	80419
no. of reflns used (R_{int})	4496 (0.0294)	5757 (0.0215)	17 997 (0.115)	18 221 (0.227)	20 822 (0.141)	26 707 (0.315)
no. of params	262	301	767	831	1003	1075
final R [$I > 2\sigma(I)$]						
R1[a]	0.0425	0.0301	0.0875	0.0682	0.0599	0.1006
wR2[b]	0.0662	0.0683	0.0939	0.1014	0.1077	0.2185
R (all data)						
R1[a]	0.0844	0.0369	0.3257	0.3189	0.2309	0.4255
wR2[b]	0.0761	0.0702	0.1223	0.1344	0.1419	0.3145
goodness of fit on F^2	0.876	0.985	0.691	0.697	0.780	0.737

[a] $R1 = \sum[|F_o| - |F_c|]/\sum|F_o|$. [b] $wR2 = \{\sum[w(F_o^2 - F_c^2)]/\sum(wF_o^2)\}^{1/2}$. $w = 1/[\sigma^2(F_o^2) + (0.075P)^2]$, where $P = [\max(F_o^2,0) + 2F_c^2]/3$.

depicted in Scheme 1, where *p*-(2,2′-dipyridylamino)-phenylboronic acid[10] was reacted with the corresponding 1,3,5-tri(*p*-bromophenyl)benzene or triazine in the prescence of $Pd(PPh_3)_4$ and NaOH. The *p*-(2,2′-dipyridylamino)phenylboronic acid was synthesized using a previously published procedure and *p*-(2,2′-dipyridylamino)-bromobenzene as the starting material.[10] These two ligands were fully characterized by NMR and elemental analyses. The Pt(II) complexes **1**−**8** were synthesized by the reactions of $[PtPh_2(SMe_2)]_n$ with the corresponding ligand of a stoichiometric amount in good yield. The relatively labile bridging SMe_2 ligand in the Pt(II) starting material was replaced by the chelating 2,2′-dipyridylamino moiety in the resulting complexes. The synthetic routes for complexes **1**−**8** are summarized in Scheme 2. Complexes **1**−**8** are stable in the solid state and in solution (except in the presence of certain halogenated solvents such as $CHCl_3$) upon exposure to air. A common problem with complexes **1**−**8** is their poor solubility in common organic solvents. Complex **1** is not soluble in common solvents such as CH_2Cl_2, CH_3CN, or DMSO, and as a result, its NMR spectrum could not be obtained. Compound **1** was characterized by elemental and single-crystal X-ray diffraction analyses. ^{1}H NMR spectra for **2**−**8** were recorded. Complex **4** is clearly fluxional in solution, as indicated by the presence of broad chemical shifts in its ^{1}H NMR spectrum. Our early investigation on starburst complexes that contain MCl_2 units (M = Pt(II), Zn(II)) chelated to the 2,2′-dipyridylamino groups revealed that this class of molecules display unusual extended structures in the solid state (e.g., polar stacked columns or hexagonal columns).[6c] To understand the origin of the fluxionality in solution and to study intermolecular interactions of complexes **1**−**8** in the solid state, single-crystal X-ray diffraction analysis on the structures of complexes became necessary. Due to the poor solubility of the complexes, it is very challenging to obtain single crystals

Scheme 2

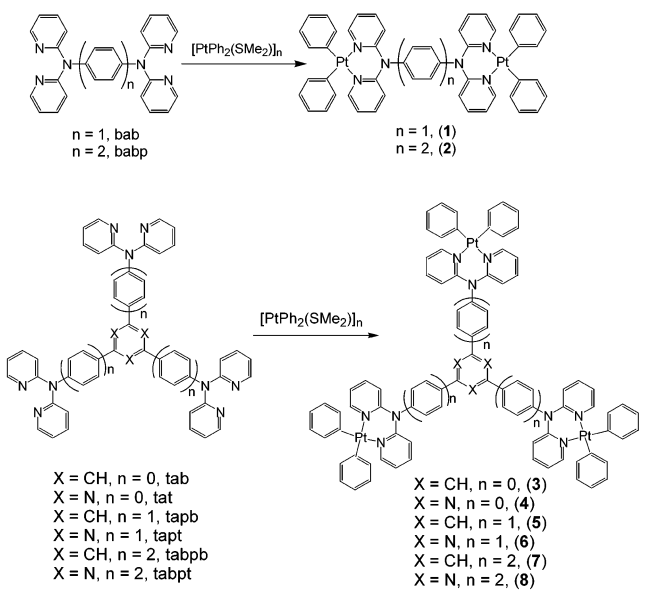

for these compounds. Various approaches were used in our effort to obtain single crystals suitable for X-ray diffraction analyses. Complexes **3** and **4** were initially precipitated out from a THF solution and were subsequently recrystallized from a CH_2Cl_2/toluene solution for **4** and a CH_2Cl_2/benzene solution for **3**. Complexes **2**, **7**, and **8** are slightly soluble in CH_2Cl_2 and THF and cannot be recrystallized. Single crystals of **2** and **8** suitable for X-ray diffraction were obtained directly from the solution containing both the free ligand and the Pt(II) starting material. For complexes **1**, **5**, and **6**, crystalline products can only be obtained by using solvent-layering techniques where the THF solution of $[PtPh_2(SMe_2)]_n$ was layered on top of the CH_2Cl_2 solution of the corresponding ligand, which upon standing at ambient temperature produced single crystals of **1** and **5** suitable for X-ray study. Various attempts to grow single crystals of complexes **6** and **7** suitable for X-ray diffrac-

(10) Jia, W. L.; Song, D.; Wang, S. *J. Org. Chem.* **2003**, *68*, 701.

Table 2. Selected Bond Length (Å) and Angles (deg) for 1−5 and 8

		Complex **1**	
Pt(1)−N(1)	2.101(5)	N(1)−Pt(1)−N(2)	83.77(19)
Pt(1)−N(2)	2.123(5)	N(1)−Pt(1)−C(7)	174.7(3)
Pt(1)−C(1)	2.009(7)	N(2)−Pt(1)−C(1)	173.1(3)
Pt(1)−C(7)	2.006(7)		
		Complex **2**	
Pt(1)−N(1)	2.111(3)	N(1)−Pt(1)−N(2)	85.13(13)
Pt(1)−N(2)	2.117(3)	N(1)−Pt(1)−C(7)	176.67(16)
Pt(1)−C(1)	2.002(4)	N(2)−Pt(1)−C(1)	175.80(13)
Pt(1)−C(7)	2.002(4)		
		Complex **3**	
Pt(1)−N(1)	2.151(13)	N(1)−Pt(1)−N(2)	86.7(6)
Pt(1)−N(2)	2.064(17)	N(1)−Pt(1)−C(37)	175.0(8)
Pt(1)−C(37)	1.985(10)	N(2)−Pt(1)−C(43)	178.1(7)
Pt(1)−C(43)	1.944(11)	N(4)−Pt(2)−N(5)	85.9(7)
Pt(2)−N(4)	2.06(2)	N(4)−Pt(2)−C(49)	177.5(8)
Pt(2)−N(5)	1.974(18)	N(5)−Pt(2)−C(55)	177.0(8)
Pt(2)−C(49)	2.037(18)	N(7)−Pt(3)−N(8)	90.2(7)
Pt(2)−C(55)	1.884(11)	N(7)−Pt(3)−C(67)	177.6(9)
Pt(3)−N(7)	1.996(17)	N(8)−Pt(3)−C(61)	179.5(6)
Pt(3)−N(8)	2.050(15)		
Pt(3)−C(61)	1.974(9)		
Pt(3)−C(67)	1.969(12)		
		Complex **4**	
Pt(1)−N(7)	2.136(13)	N(7)−Pt(1)−N(8)	85.0(6)
Pt(1)−N(8)	2.135(12)	N(7)−Pt(1)−C(34)	176.5(7)
Pt(1)−C(34)	2.053(16)	N(8)−Pt(1)−C(40)	173.7(7)
Pt(1)−C(40)	2.016(17)	N(9)−Pt(2)−N(10)	85.9(6)
Pt(2)−N(9)	2.080(14)	N(9)−Pt(2)−C(46)	176.2(7)
Pt(2)−N(10)	2.119(14)	N(10)−Pt(2)−C(52)	173.8(7)
Pt(2)−C(46)	1.918(18)	N(11)−Pt(3)−N(12)	86.0(6)
Pt(2)−C(52)	1.866(18)	N(11)−Pt(3)−C(64)	176.9(7)
Pt(3)−N(11)	2.161(13)	N(12)−Pt(3)−N(58)	176.5(7)
Pt(3)−N(12)	2.127(12)		
Pt(3)−C(58)	1.88(2)		
Pt(3)−C(64)	2.041(16)		
		Complex **5**	
Pt(1)−N(1)	2.123(9)	N(1)−Pt(1)−N(2)	84.4(4)
Pt(1)−N(2)	2.138(11)	N(1)−Pt(1)−C(55)	173.6(5)
Pt(1)−C(55)	2.025(14)	N(2)−Pt(1)−C(61)	173.5(6)
Pt(1)−C(61)	1.983(14)	N(4)−Pt(2)−N(5)	87.6(4)
Pt(2)−N(4)	2.099(10)	N(4)−Pt(2)−C(73)	177.9(5)
Pt(2)−N(5)	2.120(10)	N(5)−Pt(2)−C(67)	176.2(6)
Pt(2)−C(67)	1.980(15)	N(7)−Pt(3)−N(8)	85.2(4)
Pt(2)−C(73)	2.031(14)	N(7)−Pt(3)−C(85)	178.5(5)
Pt(3)−N(7)	2.092(11)	N(8)−Pt(3)−C(79)	176.6(7)
Pt(3)−N(8)	2.118(10)		
Pt(3)−C(79)	2.006(14)		
Pt(3)−C(85)	1.952(17)		
		Complex **8**	
Pt(1)−N(2)	2.04(2)	N(2)−Pt(1)−N(3)	86.9(10)
Pt(1)−N(3)	2.093(19)	N(3)−Pt(1)−C(76)	175.5(8)
Pt(1)−C(76)	1.888(18)	N(2)−Pt(1)−C(70)	177.1(11)
Pt(1)−C(70)	1.93(3)	N(5)−Pt(2)−N(6)	87.6(4)
Pt(2)−N(5)	2.11(3)	N(6)−Pt(2)−C(88)	177.0(14)
Pt(2)−N(6)	2.08(2)	N(5)−Pt(2)−C(82)	176.0(9)
Pt(2)−C(82)	2.00(3)	N(8)−Pt(3)−N(9)	87.7(10)
Pt(2)−C(88)	1.88(4)	N(9)−Pt(3)−C(100)	172.9(15)
Pt(3)−N(8)	2.14(3)	N(8)−Pt(3)−C(94)	179.1(13)
Pt(3)−N(9)	2.10(2)		
Pt(3)−C(94)	1.90(2)		
Pt(3)−C(100)	1.83(2)		

tion were unsuccessful. Single-crystal X-ray diffraction analyses were carried out for **1**−**5** and **8**.

Crystal Structures. The structure of complex **1** is show in Figure 1. The molecule of **1** possesses an inversion center symmetry. The Pt center is four-coordinated and adopts a typical square-planar geometry. The bab ligand bidentately chelates to two Pt(II) centers via the two 2,2′-dipyridylamino (dpa) units. Two

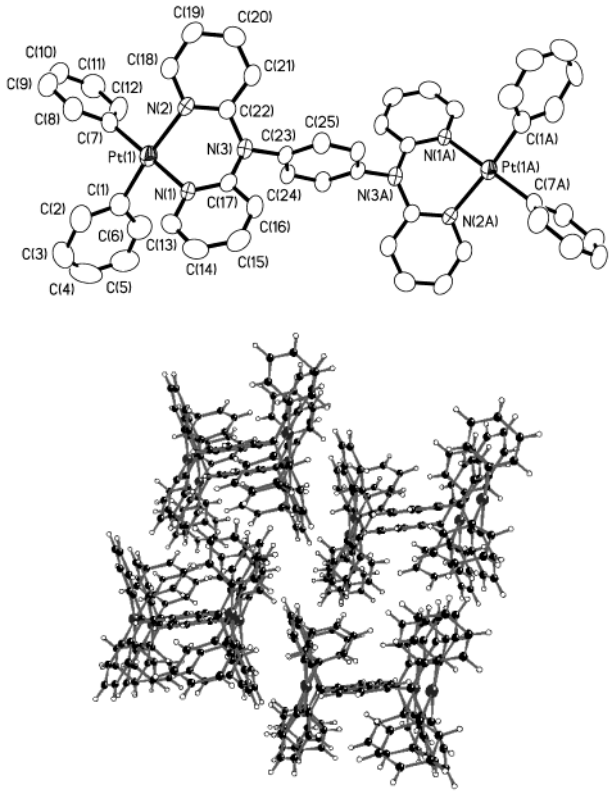

Figure 1. Top: Molecular structure of **1** with 50% thermal ellipsoids and labeling schemes. All hydrogen atoms are omitted for clarity. Bottom: Diagram showing the molecular packing of **1**.

phenyl ligands are coordinated to each Pt(II) center. The Pt−C and Pt−N bond lengths are typical for Pt(II) complexes.[1−4] The square plane of the Pt center is however a little bit distorted, as indicated by the bond angles of N(1)−Pt(1)−C(7) (174.7(3)°) and N(2)−Pt(1)−C(1) (173.1(3)°). The amino N(3) atom has a trigonal planar geometry, but its lone pair electrons are not conjugated with the central benzene ring, as indicated by the dihedral angle of the N(3)C(22)C(17) plane and the central benzene ring (98.9°). Instead, the N(3) lone pair electrons conjugate with the two pyridyl groups, as shown by their approximate coplanarity in Figure 1. This is further supported by the relatively short N(3)−C(17) and N(3)−C(22) bond lengths (1.424(8), 1.407(7) Å, respectively), compared to that of N(3)−C(23) (1.456-(7) Å). The lack of conjugation of the amino lone pair with the central benzene ring is clearly caused by nonbonding steric interactions between *ortho* hydrogen atoms of the pyridyl rings and the phenyl rings. As a consequence of the lack of conjugation of the amino N(3) atom with the central benzene ring, the two $PtPh_2$(dpa) units are oriented sideways with respect to the central benzene ring, with the two Pt atoms being coplanar with the central benzene plane. The two phenyl ligands are almost perpendicular to the Pt(1)N(1)N(2) plane (the dihedral angles between the phenyl groups and Pt(1)-N(1)N(2) plane are 76.6 and 81.8°, respectively), attributable to steric interactions between the phenyl groups and the bab ligand. The intramolecular Pt(1)−Pt(1A) separation distance is 11.576(2) Å. Molecules of **1** stack in the crystal lattice as shown in Figure 1, with the shortest intermolecular Pt(1)−Pt(1′) separation distance being 5.671(1) Å.

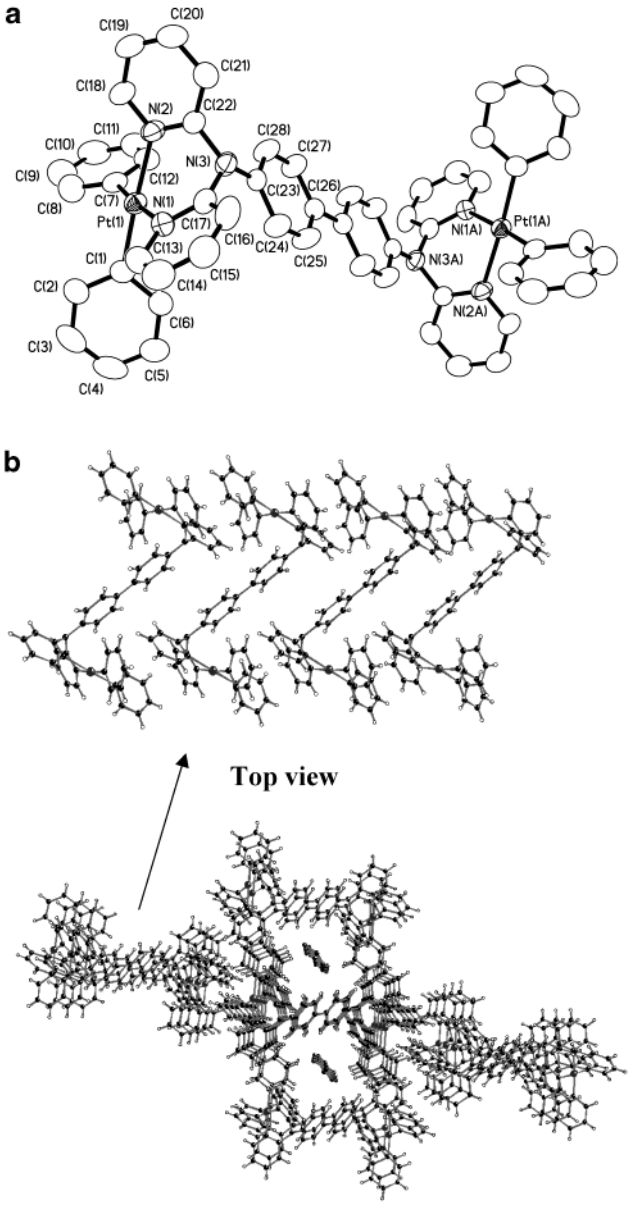

Figure 2. (a) Molecular structure of **2** with 50% thermal ellipsoids and labeling schemes. All hydrogen atoms are omitted for clarity. (b) Diagram showing molecular packing of **2** in the crystal lattice.

The structure of **2** is similar to that of **1**, as show in Figure 2a. The molecule of **2** also possesses an inversion center symmetry. The intramolecular Pt(1)−Pt(1A) separation distance is 11.916(2) Å, slightly longer than that of **1**. The central biphenyl unit is coplanar. In contrast to compound **1**, the amino nitrogen lone pair electrons in **2** appear to somewhat conjugate with the biphenyl unit, as indicated by the dihedral angle (29.4°) between the N(3)C(17)C(22) plane and the biphenyl plane, much smaller than that of **1**, and the N(3)−C(23) bond length (1.425(5) Å), much shorter than that in **1**. The two pyridyl rings of the 2,2′-dipyridylamino unit are puckered, and none of them are coplanar with the amino nitrogen atom. The dihedral angles between the two terminal phenyl rings and the Pt(1)N(1)N(2) plane are 64.3° and 58.9°, respectively. In contrast with complex **1**, the two $PtPh_2$(dpa) units chelated by the 2,2′-dipyridylamino groups in **2** are on the opposite side of the biphenyl plane, with the Pt(1) and Pt(1A) atoms being 3.042(1) Å above and below the biphenyl plane. This arrangement can be attributed to the relatively reduced nonbonding steric interactions in **2**, compared to those of **1**. In the crystal lattice of **2**, along one of the axes, the dinuclear Pt_2 units are packed in a herringbone style with the shortest intermolecular Pt(1)−Pt(1′) separation distance being 5.962(1) Å. There are no significant $\pi-\pi$ stacking interactions. THF solvent molecules are trapped in the void channels of the crystal lattice as shown in Figure 2b. These trapped THF solvent molecules are surprisingly stable and do not escape the crystal lattice at ambient temperature, as indicated by the elemental analysis results obtained for crystals at ambient temperature. TGA analysis shows that the crystals of compound **2** gradually lose the THF solvent molecule after being heated to above 40 °C (Figure 3). At about 208 °C, the loss of THF appears to be complete (∼5.7% of total weight). At this temperature, other decomposition processes also appear to take place, as indicated by the rapid weight loss above 210 °C.

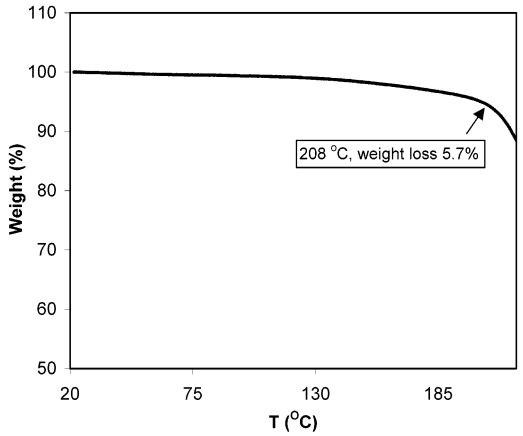

Figure 3. TGA diagram for the crystals of **2**.

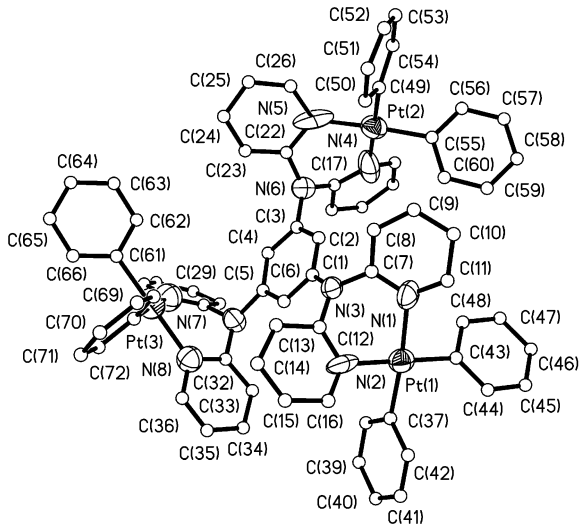

Figure 4. Molecular structure of **3** with 50% thermal ellipsoids and labeling schemes. All hydrogen atoms are omitted for clarity. All carbon atoms are shown as ideal spheres.

The structures of **3**, **4**, **5**, and **8** are shown in Figure 4, Figure 5, Figure 6, and Figure 7, respectively. The starburst ligands in these molecules are bound to three $PtPh_2$ units in the complex via the chelating

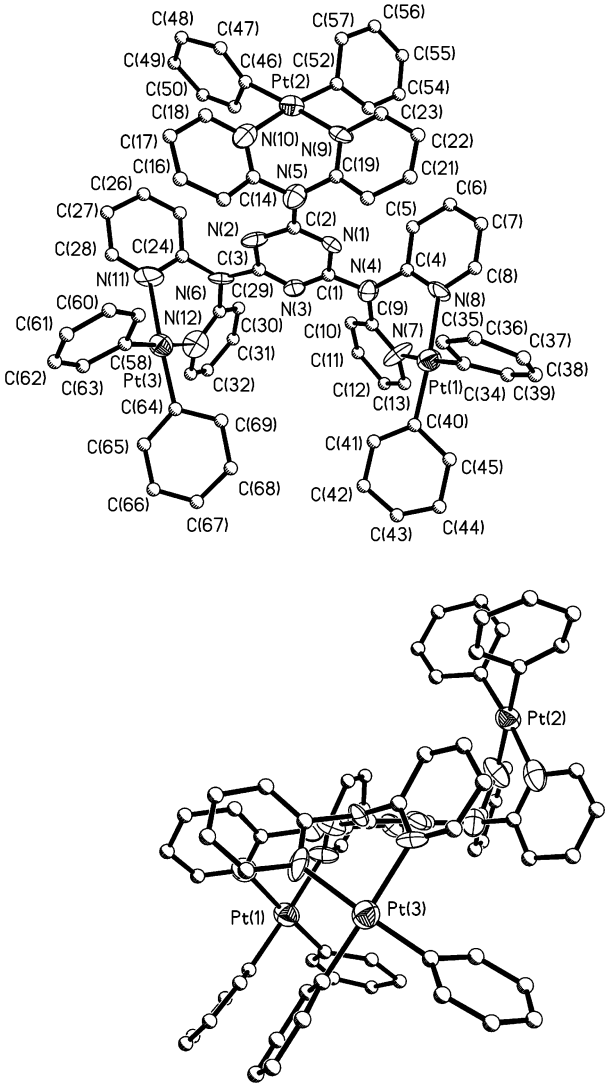

Figure 5. Top: Molecular structure of **4** with 50% thermal ellipsoids and labeling schemes. All hydrogen atoms are omitted for clarity. Carbon atoms are shown as ideal spheres. Bottom: Diagram showing the relative orientation of the $PtPh_2$(dpa) units in **4**.

2,2′-dipyridylamino (dpa) groups. The coordination environment around each Pt(II) center in these complexes is similar and resembles that of complexes **1** and **2**. The average Pt−C bond length in these complexes is 1.976 Å, and the average Pt−N bond length is 2.111 Å, slightly longer than that of Pt−C bonds.

Complexes **3** and **4** are the smallest starburst complexes, where the three $PtPh_2$(dpa) units are attached directly to the central triazine ring or the benzene ring. There are however substantial differences between the structures of **3** and **4**. In complex **4**, the amino nitrogen planes (defined by the nitrogen atom and the two adjacent carbon atoms from the two pyridyl groups) are almost coplanar with the central triazine ring, as indicated by the dihedral angles between the NC_2 planes and the triazine ring (10.5° for the N(4)C(4)C(9) plane, 13.5° for the N(5)C(14)C(19) plane, 8.5° for the N(6)-C(24)C(29) plane), an indication that the amino nitrogen lone pair electrons are conjugated with the triazine ring. This is further supported by the relatively short bond lengths of N(4)−C(1), N(5)−C(2), and N(6)−C(3) (1.377-(17), 1.370(17), and 1.349(16) Å, respectively). In contrast, the dihedral angles between the three amino NC_2 planes and the central benzene ring in **3** are 19.5° (N(3)), 85.1° (N(6)), and 21.4° (N(9)), respectively, and the N(3)−C(1), N(6)−C(3), and N(9)−C(5) bond lengths (1.370(18), 1.452(19), and 1.519(19) Å, respectively) are substantially longer than the corresponding ones in **4**, which indicates either substantial loss of conjugation or no conjugation by the amino nitrogen lone pair electrons with the central benzene ring. The loss of conjugation is most pronounced for the N(6) atom, where the N(6)C(18)C(22) plane is almost perpendicular to that

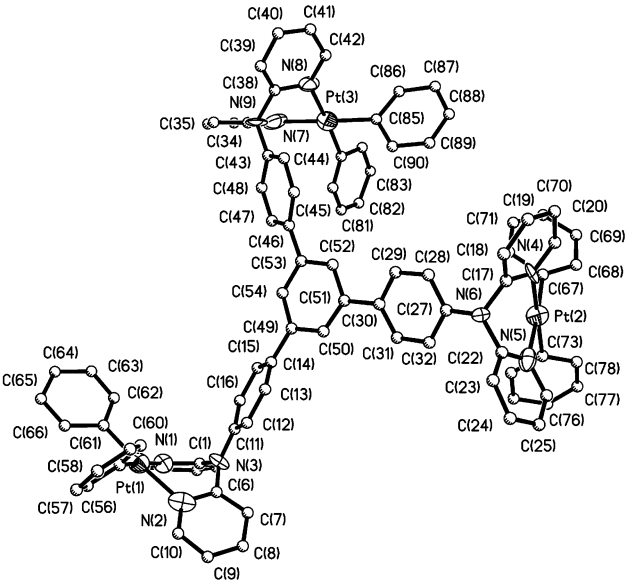

Figure 6. Molecular structure of **5** with 50% thermal ellipsoids and labeling schemes. All hydrogen atoms are omitted for clarity. Carbon atoms are shown as ideal spheres.

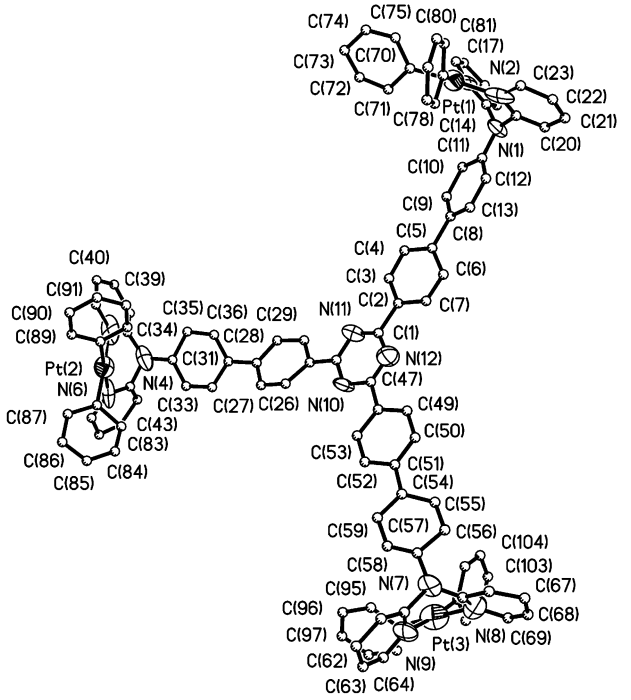

Figure 7. Molecular structure of **8** with 50% thermal ellipsoids and labeling schemes. All hydrogen atoms are omitted for clarity. Carbon atoms are shown as ideal spheres.

Chart 1

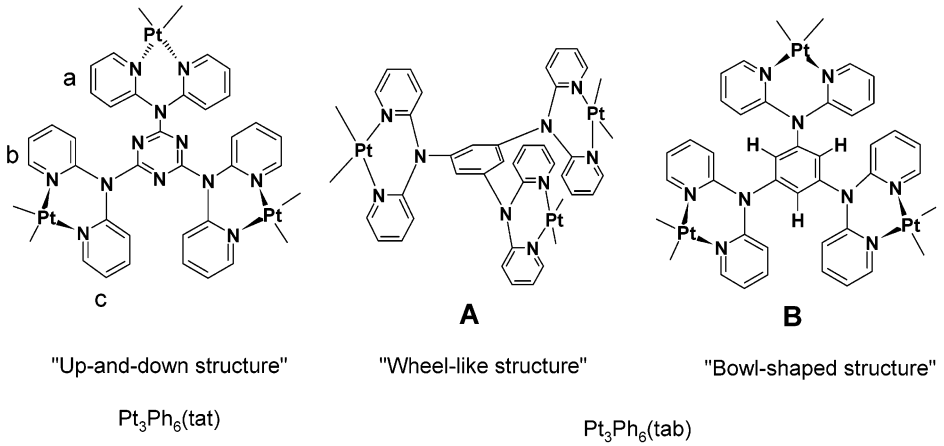

of the central benzene ring. As a consequence, the Pt(2) unit in **3** is neither above nor below but is oriented sideways with respect to the central benzene ring in the same manner as the $PtPh_2$(dpa) units in **1**. The remaining two $PtPh_2$(dpa) units in **3** are somewhat oriented sideways and are on the opposite sides of the central benzene plane. The shortest Pt−Pt separation distance is intramolecular, 7.695(2) Å between Pt(1) and Pt(2). The loss of conjugation of the amino nitrogen lone pair electrons with the central benzene ring in **3** can be again attributed to steric interactions between the *ortho* hydrogen atoms. In compound **4**, due to the conjugation of the amino nitrogen lone pair electrons with the triazine ring, the three $PtPh_2$(dpa) units are oriented above and below the triazine plane, two of which (Pt(1) and Pt(3)) are below the plane of the triazine ring, and the remaining one is above the triazine plane (Figure 3, bottom and Chart 1). A symmetric arrangement where all three Pt units are on the same side with respect to the central triazine (or benzene) plane has been observed in Pt_3Cl_6(tab) and Pt_3Cl_6(tat) complexes reported previously, which display a bowl-shaped structure in the solid state, stabilized by intermolecular electrostatic interactions between the chloride ligands and the hydrogen atoms of the bab or tat ligand.[6c] The lack of a symmetric structure similar to that of Pt_3Cl_6(tat) by **4** can be attributed to nonbonding steric interactions between the phenyl groups and the tat ligand. The planes of the Pt(1) unit and the Pt(3) unit in **4** are not completely parallel, with a dihedral angle of 56.6°. The intramolecular Pt(1)−Pt(3), Pt(1)−Pt(2), and Pt(2)−Pt(3) separation distances are 8.150(2), 8.726(2), and 8.285(2) Å, respectively, which are much shorter than those of **1** and **2**. The shortest intermolecular Pt−Pt separation distance is 6.980(2) Å between Pt(1) and Pt(2A).

The three $PtPh_2$(dpa) units in **5** are attached to a 1,3,5-tri(*p*-phenyl)benzene unit which is not coplanar, as indicated by the dihredral angles between the three phenyl rings and the central benzene ring (12.3°, 32.0°, and 40.4°, respectively). With respect to the 1,3,5-tri(*p*-phenyl)benzene unit, Pt(2) and Pt(3) are on one side while the Pt(1) unit is on the opposite side. However, these $PtPh_2$(dpa) units are all somewhat rotated sideways and not exactly above or below the central aromatic linker, resembling those in **3**. Figure 6 shows that unlike compounds **3** and **4**, there is sufficient space in **5** for all three $PtPh_2$(dpa) groups to be on the same side with respect to the central aromatic unit. The fact that the three $PtPh_2$(dpa) groups in **5** are not on the same side is clearly not due to intramolecular interactions but intermolecular interactions or molecular packing in the solid state. The shortest Pt−Pt separation distance is intermolecular, 6.980(2) Å, between Pt(1) and Pt(3′). The shortest intramolecular Pt−Pt separation distance is ∼11.8 Å between Pt(2) and Pt(3), similar to that of **2**, but much longer than those of **3** and **4**, attributable to the exta phenyl group between the central benzene ring and the dpa moiety. There are intermolecular $\pi-\pi$ stacking interactions between the central 1,3,5-tri(*p*-phenyl)benzene units with the shortest atomic separation distance being 3.86 Å.

The three $PtPh_2$(dpa) units in **8** are attached to a 2,4,6-tris(biphenyl)-1,3,5-triazine unit as shown in Figure 7. As a consequence, the intramolecular Pt−Pt separation distances are very long, with the Pt(2)−Pt(3) distance being the shortest (18.70(1) Å). Two of the three biphenyl units are not planar, as indicated by the dihedral angles between phenyls (2.2°, 14.7°, and 11.1°, respectively). The three $PtPh_2$(dpa) units are orientated somewhat sideways with respect to the central aromatic linker, in a manner similar to that observed in **5**. This arrangement of the three Pt units in **8** is clearly due to the presence of the biphenyl unit between the triazine ring and the dpa group that significantly reduces intramolecular steric interactions. The shortest Pt−Pt separation distance is intermolecular, 5.908(2) Å, between Pt(3) and Pt(3′). Some $\pi-\pi$ stacking interactions between the central aromatic units are observed.

Structures and Fluxionality in Solution. On the basis of the crystal structures, we believe that the starburst molecules of **5**−**8** should have symmetric structures with an approximate C_3 symmetry in solution since there is sufficient space for the three $PtPh_2$(dpa) units to orient in any direction. The most likely structures for **5**−**8** in solution are propellers with all three $PtPh_2$(dpa) units being oriented somewhat sideways in the same direction, resembling the structures of $(ZnCl_2)_3$(tapb) and $(ZnCl_2)_3$(tapt) molecules, which have a rigorous C_3 symmetry.[6c,d] Indeed, ^{1}H NMR spectra of complexes **5**−**8** display only one set of chemical shifts, corresponding to the $PtPh_2$(dpa) units, and no fluxional phenomena were observed for these complexes, indicat-

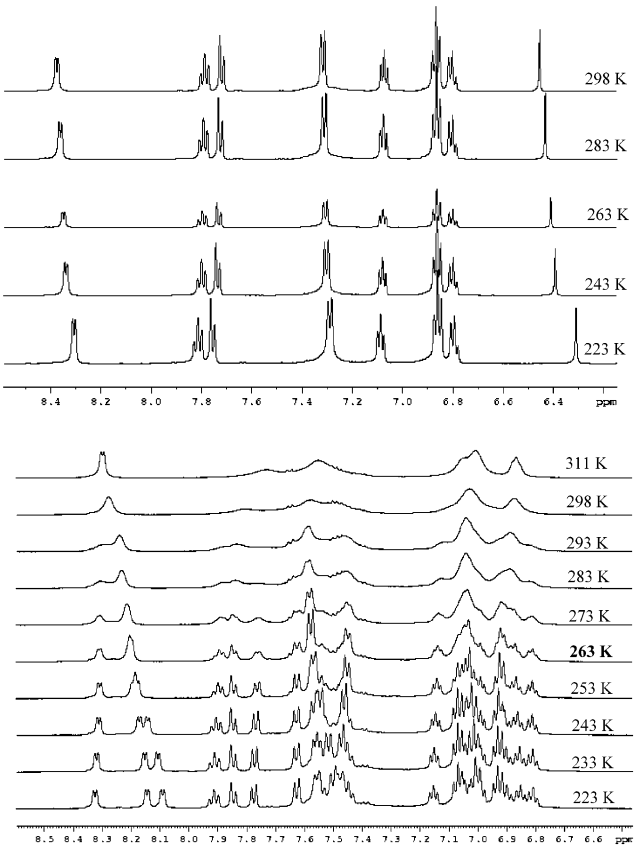

Figure 8. Variable-temperature ^{1}H NMR spectra. Top: compound **3**. Bottom: compound **4**.

ing that they do have a symmetric structure in solution. No fluxional behavior was observed for compounds **1** and **2**.

In contrast, compounds **3** and **4** are very crowded molecules, and there is not sufficient space to allow all three $PtPh_2$(dpa) groups to be oriented in the same direction, above or below the central aromatic ring. Consequently, one would anticipate that in solution **3** and **4** retain the same structures as in the solid state, e.g., the "up-and-down" structure shown in Chart 1, where not all three $PtPh_2$(dpa) units have the same environment. ^{1}H NMR experiments appear to confirm that this is the case for compound **4**, which displays temperature-dependent ^{1}H NMR spectra, consistent with the presence of a dynamic exchange process. As shown in Figure 8, bottom, at ambient temperature, the ^{1}H NMR spectrum of **4** shows broad peaks corresponding to one set of $PtPh_2$(dpa) chemical shifts, an indication of the presence of a relatively slow exchange process. Raising the temperature to 311 K, the spectrum becomes somewhat better resolved but remains broad. As the temperature is decreased, the spectrum gradually becomes sharp. At 243 K, well-resolved peaks corresponding to three different sets of pyridyl groups in a 1:1:1 ratio are observed. Three sets of phenyl chemical shifts are also observed at 243 K. As shown by Figure 5 and Chart 1, the molecule of **4** has an approximate mirror plane symmetry relating the Pt(1) unit to the Pt(3) unit, resulting in two different sets of Pt environments and three different sets of pyridyl rings (labeled as **a**, **b**, and **c**, respectively in Chart 1) and three different sets of phenyl groups as well. The low-temperature ^{1}H NMR spectrum is therefore consistent

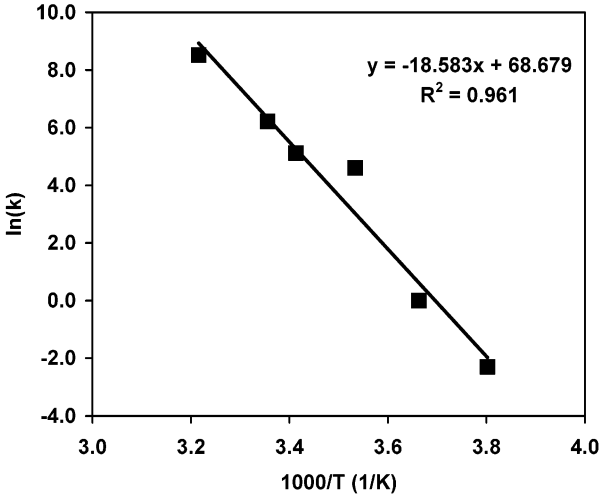

Figure 9. Arrhenius plot of ln(k) versus 1/T for compound **4** and the best fit.

with the structure of **4** observed in the solid state. NMR data lead us to conclude that the three different sets of pyridyl groups (as well as the phenyl groups) undergo slow exchange in solution at ambient temperature caused by the orientation interconversion of the three $PtPh_2$(dpa) units with respect to the triazine plane. Using a two-site exchange model with a population ratio of 1:2 for the two sites and the variable-temperature NMR data, we calculated a series of rate constants at different temperatures. Using these rate constants and the corresponding temperatures and the Arrhenius plot shown in Figure 9, we estimated that the activation energy for the exchange process of **4** is ~154(10) kJ mol^{-1}. This rather large activation energy can be attributed to the presence of significant intramolecular steric interactions in **4** that must be overcome in order to achieve the up-and-down orientation interconversion.

One surprising finding is that a similar fluxional behavior was not observed for compound **3**. Through the temperature range 223−298 K, the pattern of the ^{1}H NMR spectrum of **3** remains the same and corresponds to one set of $PtPh_2$(dpa) unit and one proton from the central benzene ring (Figure 8, top), a clear indication that **3** has a symmetric structure in solution with all $PtPh_2$(dpa) units being in the same environment. To achieve a symmetric structure, only two arrangements are possible, **A** and **B** as depicted in Chart 1. In structure **A**, all three $PtPh_2$(dpa) units are oriented sideways with the three Pt atoms being coplanar with the central benzene plane, and there is no conjugation between the amino nitrogen lone pair and the central benzene, resulting in a wheel- or paddle-like arrangement similar to that observed in compound **1**. In structure **B**, all three $PtPh_2$(dpa) units are above (or below) the central benzene ring with a bowl shape similar to that of $(PtCl_2)_3$(tab) or $(PtCl_2)_3$(tat), and the amino nitrogen lone pair electrons are conjugated with the central benzene ring. Clearly, due to steric interactions, the bowl-shaped structure **B** is not favorable for **3**. We therefore believe that compound **3** adopts the wheel-like structure **A** in solution where all three Pt atoms have the same environment. The crystal structure of **3** shows that the amino nitrogen lone pair electrons do not favor conjugation with the central benzene ring due to steric interactions. In contrast, the

Table 3. Luminescence Data for Compounds 1−8, tabpb, and tabpt

compd	UV−vis, nm[a] (ϵ/M^{-1} cm^{-1})	excitation wavelength, nm	emission (λ_{max}, nm)	decay lifetime (τ, ms)[c]	conditions
1	N/A	375	473	0.00969(6)	solid, 298 K
			509	0.01204(4)	
			540 (sh)	0.0136(1)	
2	232 (99 130)	381	486	1.352(2)	CH_2Cl_2, 77 K
	280 (30 772)		518 (sh)[b]	1.358(2)	
	304 (66 890)	395	481	0.0378(2)	solid, 298 K
			519	0.0374(3)	
			560 (sh)	0.0392(8)	
3	240 (378 270)	378	460	0.305(6)	CH_2Cl_2, 77 K
	314 (70 410)				
	370 (29 560)				
4	232 (142 720)	387	496	0.160(4)	CH_2Cl_2, 77 K
	270 (99 400)				
	362 (21 070)				
5	232 (227 580)	376	402		CH_2Cl_2, 77 K
	276 (197 170)		**470**	**1.596(9)**	
	336 (89 570)		**500 (sh)**	**1.506(8)**	
6	232 (126 310)	377	423		CH_2Cl_2, 77 K
	314 (76 180)		**472**	**2.06(2)**	
	352 (93 130)		**508 (sh)**	**1.94(4)**	
7	230 (191 500)	395	**511**	**2.56(4)**	CH_2Cl_2, 77 K
	306 (216 620)		**542**	**2.48(5)**	
8	232 (148 730)	395	463		CH_2Cl_2, 77 K
	334 (132 500)		**522**	**2.27(4)**	
	352 (130 060)		**555**	**2.15(8)**	
tabpb	230 (42 130)	341	399		solid, 298 K
	282 (28 320)	342	404		CH_2Cl_2, 298 K
	316 (14 700)	358	400		CH_2Cl_2, 77 K
		358	**506**	**4.22(7)**	**CH_2Cl_2, 77 K[d]**
			538 (sh)	**4.01(5)**	
tabpt	232 (28 890)	368	469		solid, 298 K
	284 (49 460)	398	484		CH_2Cl_2, 298 K
	358 (50 330)	395	452		CH_2Cl_2, 77 K
		395	**525**	**4.06(3)**	**CH_2Cl_2, 77 K[d]**
			562	**3.86(6)**	

[a] All data were collected for CH_2Cl_2 solution ([M] = 2.2×10^{-6} to 4.6×10^{-6}) at ambient temperature. [b] sh = shoulder. [c] A reliable lifetime could not be obtained for the fluorescent emission due to the limitation of the instrument, which cannot measure lifetimes in the nanosencond regime. [d] Obtained using a time-resolved phosphorescent spectrometer.

amino nitrogen lone pair conjugation with the triazine ring is favored in compound **4**, due to the lack of *ortho* hydrogen atoms on the triazine ring and the presence of the three electronegative nitrogen atoms on the triazine. Consequently, in solution compound **4** favors the "up-and-down" structure similar to the crystal structure, not the wheel-like structure **A**.

Luminescent Properties. Upon irradiation by UV light, the free ligands bab, babp, tab, tat, tapb, tapt, tabpb, and tabpt display an intense blue fluorescent emission in solution and the solid state at ambient temperature with the emission maximum at 400, 415, 433, 415, 440, 410, 404, and 484 nm, respectively. In contrast to the free ligands, all Pt(II) complexes do not show detectable emission in solution at ambient temperature. Bluish green emission (λ_{max} = 473, 509 nm for **1**; λ_{max} = 481, 519 nm for **2**) was however observed in the solid state for complexes **1** and **2** at ambient temperature. At 77 K, the frozen solutions of all complexes except **1** (due to the insolubility of **1** in organic solvents, its emission spectra in solution could not be recorded) exhibit bright blue-green emission with the emission maximum shifted to a much longer wavelength, compared to those of the free ligands at ambient temperature (see Table 3). The emission spectra of the complexes at 77 K appear to be dominated by phosphorescence of the ligands because of their resemblance with the phosphorescent emission spectra of the corresponding free ligands. (The free ligands display a weak phosphorescent emission at 77 K in solution, detectable by a time-resolved phosphorescent spectrometer.) For complexes **5**, **6**, and **8**, weak fluorescent emissions at λ_{max} = 402, 423, and 463 nm, respectively, were also observed at 77 K, attributable to ligand-centered emission. For the remaining complexes, no significant fluorescent emission was detected. As two representative examples, the full emission spectra of complexes **7** and **8** at 77 K in CH_2Cl_2 matrix and the phosphorescent spectra of the corresponding free ligands obtained by using time-resolved phosphorescent spectrometry are shown in Figure 10. The resemblance of the emission spectra of the complexes with those of the free ligands is obvious. Emission lifetime measurements for the complexes at 77 K in a frozen solution revealed that the emission bands (excluding the fluorescent bands) from the complexes have decay lifetimes in the regime of phosphorescence and are much shorter than those of the corresponding free ligands. For example, the free babp ligand has a green phosphorescent emission band with the maximum at 486 and 520 nm at 77 K in solution. This emission band has a decay lifetime in the seconds range such that the green emission was visible by eye for a few seconds after the excitation source was switched off. Due to its extremely long decay time, we could not measure it accurately. In contrast, the complex Pt_3Ph_6(babp) (**2**) has a green emission in the same region, but with a much shorter decay time (1.35 ms) than that of the free ligand. The impact of the Pt(II)

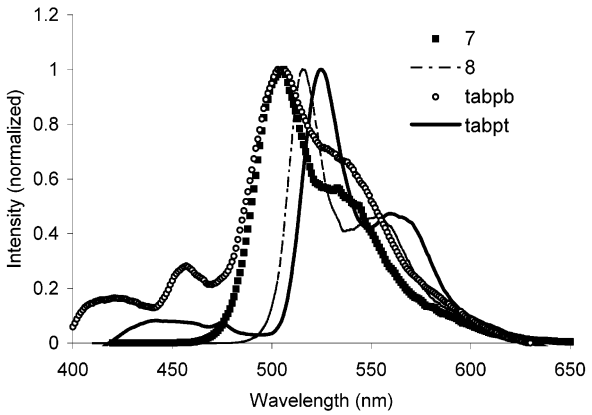

Figure 10. Emission spectra of **7** and **8** at 77 K in CH_2Cl_2 and the phosphorescent emission spectra of the free ligands tabpb and tabpt in CH_2Cl_2 solution at 77 K obtained using a time-resolved phosphorescence spectrometer.

center on the phosphorescent emission of the ligand therefore appears to be 2-fold: (a) the Pt(II) center quenches the fluorescent emission and enhances the phosphorescent emission of the ligand, (b) the Pt(II) center substantially decreases the phosphorescent decay time of the ligand. This impact appears to diminish with the size increase of the ligand. For example, the two biggest ligands, tabpb and tabpt, have green phosphorescent emission bands (λ_{max} = 506 nm, 538 nm for tabpb; 525 nm, 562 nm for tabpt) with a decay lifetime of 4.1(1) and 3.9(1) ms, respectively, while the corresponding emission of the complexes **7** and **8** (λ_{max} = 511 nm, 542 nm for **7**; 522 nm, 555 nm for **8**) has a decay lifetime of 2.0(1) and 2.5(1) ms, respectively. The decrease of the decay lifetime of ligands in **7** and **8** compared to those of the free ligands is not as dramatic as those of the smaller complexes such as **2**. On the basis of the above observations, we can conclude that the emission of the complexes is ligand-based, involving most likely $\pi \rightarrow \pi^*$ transitions. (In the case of triazine derivatives, charge transfer between the dipyrdiylamino unit and the electronegative triazine ring is also likely.) The striking difference between the free ligands and the complexes is that the phosphorescent emission of the complexes is much more bright and easily detectable than the phosphorescent emission of the free ligands. Furthermore, the emission of the free ligands is dominated by fluorescence, but the emission of the complexes is nearly exclusively phosphorescence. Clearly the Pt(II) centers in the complexes played a key role in enhancing the phosphorescent emission of the ligands. Similar enhancement of ligand-based phosphorescent emission by the Pt(II) center in porphyrin derivative Pt(II) complexes has been attributed to the bright emission and their successful uses as emitters in OLEDs.[4] The absence of emission in the solid state by complexes **3**−**8** can be attributed to intermolecular quenching. To minimize intermolecular quenching, we doped our complexes into a rigid polymer matrix such as PVK. However, no luminescence from the complexes was observed in the doped polymers at ambient temperature, attributable to thermal quenching due to the long decay lifetimes, which makes this class of Pt(II) complexes not useful as emitters in OLEDs.

In summary, eight new neutral binuclear and starburst trinuclear platinum complexes of 2,2′-dipyridylamino derivative ligands as well as two new blue luminescent starburst ligands have been synthesized. The emission of the Pt(II) compounds is dominated by phosphorescent emissions that cover the region of blue to green and can be attributed to ligand-based transitions. The Pt(II) atoms in the complexes play a key role in promoting phosphorescent emissions. These new complexes display versatile structures in solution and the solid state, where the conjugation of the amino nitrogen lone pair of the dpa unit with the central aromatic unit of the ligand and steric interactions play an important role. Although these new complexes are not useful in OLEDs, they do show interesting reactivity toward C−Cl bonds when exposed to light and may be useful in photochemical reactions, which are being investigated in our laboratory.

Acknowledgment. We thank the Natural Sciences and Engineering Research Council of Canada for financial support.

Supporting Information Available: Complete X-ray diffraction data for **1**−**5** and **8**, including tables of atomic coordinates, thermal parameters, bond lengths and angles, and hydrogen parameters, and complete luminescent spectra of **1**−**8**. This material is available free of charge via the Internet at http://pubs.acs.org.

OM030262K